



Diagnosis of Solar Water Heaters Using Solar Storage Tank Surface Temperature Data

Preprint

J. Burch and L. Magnuson
National Renewable Energy Laboratory

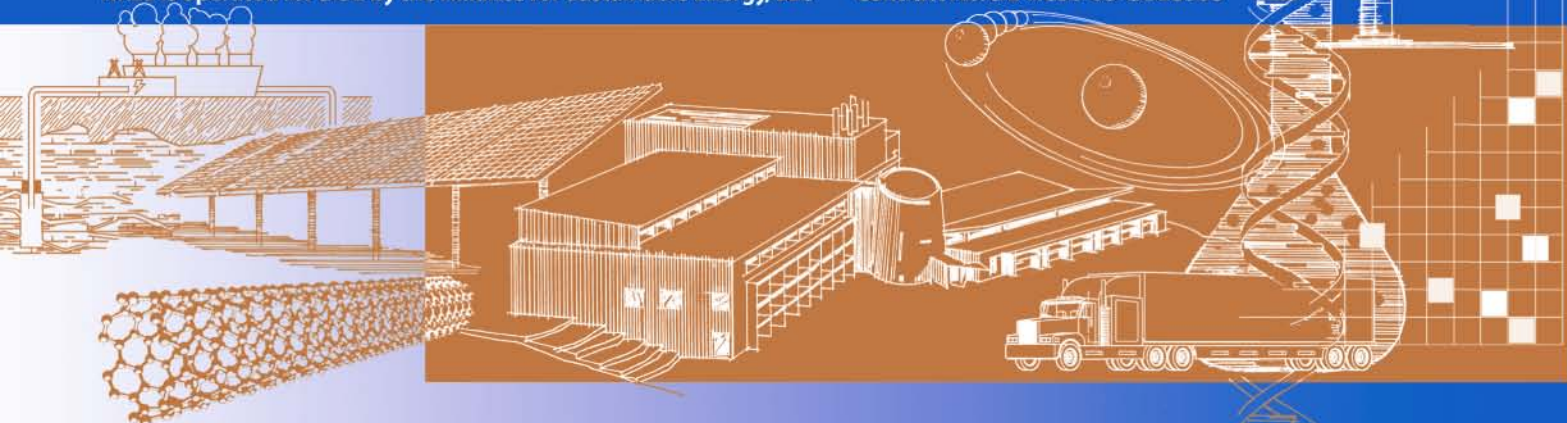
G. Barker
Mountain Energy Partnership

M. Bullwinkel
State University of New York at Canton

*To be presented at the American Solar Energy Society (ASES)
2009 National Solar Conference (SOLAR 2009)
Buffalo, New York
May 11–16, 2009*

Conference Paper
NREL/CP-550-45465
April 2009

NREL is operated for DOE by the Alliance for Sustainable Energy, LLC Contract No. DE-AC36-08-GO28308



NOTICE

The submitted manuscript has been offered by an employee of the Alliance for Sustainable Energy, LLC (ASE), a contractor of the US Government under Contract No. DE-AC36-08-GO28308. Accordingly, the US Government and ASE retain a nonexclusive royalty-free license to publish or reproduce the published form of this contribution, or allow others to do so, for US Government purposes.

This report was prepared as an account of work sponsored by an agency of the United States government. Neither the United States government nor any agency thereof, nor any of their employees, makes any warranty, express or implied, or assumes any legal liability or responsibility for the accuracy, completeness, or usefulness of any information, apparatus, product, or process disclosed, or represents that its use would not infringe privately owned rights. Reference herein to any specific commercial product, process, or service by trade name, trademark, manufacturer, or otherwise does not necessarily constitute or imply its endorsement, recommendation, or favoring by the United States government or any agency thereof. The views and opinions of authors expressed herein do not necessarily state or reflect those of the United States government or any agency thereof.

Available electronically at <http://www.osti.gov/bridge>

Available for a processing fee to U.S. Department of Energy and its contractors, in paper, from:

U.S. Department of Energy
Office of Scientific and Technical Information
P.O. Box 62
Oak Ridge, TN 37831-0062
phone: 865.576.8401
fax: 865.576.5728
email: <mailto:reports@adonis.osti.gov>

Available for sale to the public, in paper, from:

U.S. Department of Commerce
National Technical Information Service
5285 Port Royal Road
Springfield, VA 22161
phone: 800.553.6847
fax: 703.605.6900
email: orders@ntis.fedworld.gov
online ordering: <http://www.ntis.gov/ordering.htm>



DIAGNOSIS OF SOLAR WATER HEATERS USING SOLAR STORAGE TANK SURFACE TEMPERATURE DATA

Jay Burch and Lee Magnuson
National Renewable Energy Laboratory
1617 Cole Blvd.
Golden, CO 80401
jay.burch@nrel.gov

Greg Barker
Mountain Energy Partnership
13900 N. 87th St.
Longmont, CO 80503

Matt Bullwinkel
State University of New York at Canton
34 Cornell Drive
Canton, NY 13617

ABSTRACT

Based on the tank energy balance, net gain into the solar storage tank can be inferred from the time derivative of the average tank temperature. Using temperature at the tank wall under insulation as a surrogate for fluid temperature, sensor mounting is simple and the inferred gains are useful for solar water heater (SWH) diagnostics. Positive daytime gain is compared to solar gain computed from site-specific parameters for an assumed clear day. The solar storage tank loss coefficient is inferred from temperature decay at night, and is compared to the value computed from tank description. Larger draws are evident as sharp drops in storage temperature. Analyses are embodied in a tool validated against directly-measured gains. Inoperative single-family SWH are easily detected, signaling need for repair. Detection of system control issues and shading are exemplified. In large multi-family systems, frequent daytime draws will bias the comparison to expected solar gain.

1. INTRODUCTION

Diagnostic monitoring is taken here as determination from short-term data if a solar water heater (SWH) is operating correctly. To be routinely applied, it should be inexpensive and easy, especially if intended for small domestic SWH. Many diagnostic methods exist based on the wide range of possible data and allowed expense (1,2); we focus here on improving a method based on the solar storage tank surface temperatures (3). Tank surface temperature can usually be easily accessed, and when insulated it is a good surrogate for the nearby fluid temperature. Significant temperature rise on some days shows that a SWH is operating. Quantitative analysis using the tank as a calorimeter can indicate *how well* the entire system is performing, by

comparing measured gain to expected operation. In (3), *daily total* net energy gain computed from the tank temperature rise was compared to gain computed for site-specific parameters under no-draw, clear sky conditions. However, there are often daytime draws, lowering net gain and biasing the comparison. In this paper, the inferred net gain and expected clear-day solar gains are compared dynamically as *rates* throughout the day. If draws are detected as low or negative dT_{tank}/dt , then the comparison is not done using that period. This minimizes the effect of (unmonitored) draws on the comparison of net to expected solar gain, and increases the odds of getting some clear-sky/no-draw conditions during the monitoring.

The work here is different from previous studies using tank surface temperatures (4,5). In those methods, a system characterization was derived that allowed accurate projection of annual performance. Complete weather data including solar incidence is needed. The system must be isolated, with no draws. Here, weather data are not needed, and the system operates normally with draws. Compared to previous diagnostic methods (1,2), the method here is simple and low-cost. Compared to (2), this method has lower accuracy and diagnostic power. It can be implemented in controllers as a software option, notifying the owner when performance is sub-par. Another application is low-cost, large-scale screening via mail-in procedures, locating malfunctioning systems to be repaired and yielding overall reliability data on systems. Combined with subsequent repair data from partnering refurbishment firms, component failure rates could also be determined. The analysis algorithms are developed in Section 2. The algorithms have been embodied in a spreadsheet available for download (6). The method is applied to both residential and multi-family SWH in Section 3, with conclusions in Section 4.

2. THEORETICAL BASIS

The “tank-as-calorimeter” method presented here is based upon the energy balance shown schematically in Fig. 1. With the control volume taken around the tank, the instantaneous energy balance is:

$$dQ_{\text{tank}}/dt = \sum_i dQ_i/dt = dQ_{\text{solar}}/dt - dQ_{\text{loss}}/dt - dQ_{\text{draw}}/dt. \quad (1)$$

where Q_{tank} is given as $C_{\text{tank}}T_{\text{tank,avg}}$, and $T_{\text{tank,avg}}$ is the capacitance-weighted average temperature, and C_{tank} is calculated as $\rho_{\text{wtr}}c_{p,\text{wtr}}V_{\text{tank}}$. Here, dT_{tank}/dt is computed directly from differencing the tank temperature data. The choice of time step to compute the derivative is user-controlled, useful to minimize noise when the data interval is perhaps too small. Tank loss is computed as

$$dQ_{\text{tank,loss}}/dt = UA_{\text{tank,est}}(T_{\text{tank,avg}} - T_{\text{env}}). \quad (2)$$

For a practical method, plumbing should not be breached. Here, the sensors are to be mounted on the surface of the tank, as indicated in Fig. 2. It is important that the sensor be under the tank wall insulation to keep its reading close to the tank fluid temperature. A simple resistor chain argument shows that the difference between the tank wall temperature and the tank fluid is typically $< 0.1^\circ\text{C}$, sufficient for the modest accuracy of the method here. Surface-mount sensors compared well with immersed sensors in (5).

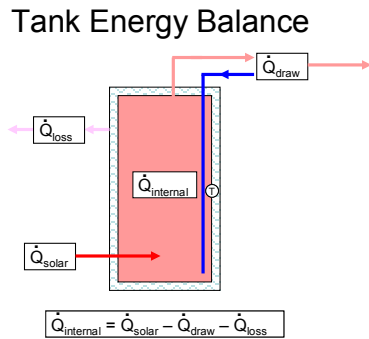


Fig. 1. Schematic tank energy balance and surface temperature measurement.

In using the tank energy balance for calorimetry, the problem becomes how to separate the terms in the sum ($Q_{\text{solar}} - Q_{\text{loss}} - Q_{\text{draw}}$). By taking dynamic data, times when a specific term is dominant can be separated in time, as illustrated in Fig. 3. Solar gains are evident as positive derivatives, and losses are evident at night. Draws are important, and it is clearly desirable to know when they are occurring. When the draw is significant compared to the tank’s thermal capacitance and the tank is well-mixed, the draw manifests as a sharp drop in $T_{\text{tank,avg}}$, as in Fig. 3 and in single-family data below. In most SWH in the U.S., flow rates on the tank side are large enough that the tank stays

well-mixed. Draws can be undetectable at night when pumps are not mixing the tank. Draws will be often undetected in well-stratified, low-flow systems common in Europe, and the data may only show when the thermocline passes the sensor location. Draws can be undetectable in large multi-family systems where there are frequent draws that are in net smaller than the net solar gain into the tank.

Surface Mount Detail

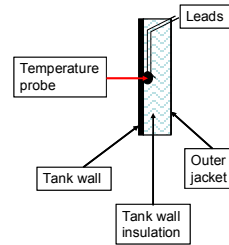


Fig. 2. The tank surface probe should be well-insulated.

Table 1 shows expected accuracy of the flux inference. Accuracy of $\sim 3\%$ can be attained when $T_{\text{tank,avg}}$ is accurately measured and C_{tank} is well-known (7). The key uncertainty is how well one or more surface temperatures represent $T_{\text{tank,avg}}$. In systems with high flow during solar operation that are typical in U.S. design, the tank is turned over rapidly ($V_{\text{tank}}/m_{\text{dot,tank}} \ll 1/\text{hr}$ and is reasonably well-mixed. In this case, a single surface temperature represents the average to within a few $^\circ\text{C}$, implying about 10% accuracy at peak operation. Solar tanks can remain stratified during operation, however, as with low-flow systems in Europe where ($V_{\text{tank}}/m_{\text{dot,tank}} \ll 10 \text{ hr}$). Accuracy degrades severely in this case unless 3 or more probes are used.

TABLE 1. ACCURACY OF TANK CALORIMETRY

Measurement	$\delta T_{\text{tank,avg}}$	$\delta Q_{\text{dot,tank}}/Q_{\text{dot,tank}}$
Line-averaging RTD	0.5°C	3%
Surface temp, well-mixed	2°C	$\sim 15\%$
Surface temp, stratified	$\sim 20^\circ\text{C}$	$\sim 100\%$
3 Surface temp, stratified	2°C	$\sim 15\%$

Temperatures on Sunny Day with draws

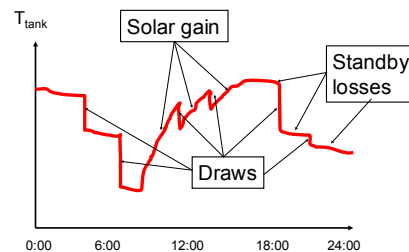


Fig. 3. Schematic tank temperature vs. time, showing periods of solar gain, draws, and standby losses.

2.1 Parameter inference

Assuming no draw, Eqn. 1 implies that solar gains are $dQ_{\text{solar}}/dt = dQ_{\text{tank}}/dt + dQ_{\text{loss}}/dt$. Losses are computed with the computed value of UA_{tank} . Pump on/off times are taken as the first/last positive dT_{tank}/dt . The tank loss coefficient UA_{tank} is inferred from the tank temperature decay at night, when no draws are expected. The tank UA is calculated from the well-known expression:

$$UA_{\text{tank}} = C_{\text{tank}} \ln[(T(t_{\text{beg}}) - T_{\text{env}})/(T(t_{\text{end}}) - T_{\text{env}})] / (t_{\text{end}} - t_{\text{beg}}) \quad (5)$$

where t_{beg} , t_{end} are beginning and ending times of the decay. The user sets an invariant time window for analyzing decay. T_{env} may be estimated, but it should be measured if more precision in inference is needed, as when one wants to detect night-time thermosiphoning. T_{env} is particularly difficult to estimate when the tank is in a garage or other unconditioned space.

2.2 Comparison of inferred parameters to expectation

Useful solar gain on a clear day is calculated as

$$dQ_{\text{coll,clr}}/dt = A_{\text{coll}} [F_r(\tau\alpha)_n K_{\text{IAM}}(\theta) I_{\text{coll,clr}} - F_r U_l (T_{\text{coll,in}} - T_{\text{amb}})] \quad (4)$$

where $F_r(\tau\alpha)_n/F_r U_l$ are the measured collector gain/loss coefficients in the well-known collector efficiency equation. These values have to be corrected for off-test flow rate, series array configuration, piping losses, and heat exchanger penalty, as described in (7). These corrections are typically not large for small-scale systems, but can become important for large, multi-family systems, especially the piping loss term. An example is shown in Section 3.3. Table 2 lists inputs and data sources for the calculations used here.

$I_{\text{coll,clr-day}}$ depends on site latitude, longitude, elevation, and collector orientation. Calculations here use the methods laid out in (8), based on correlations for beam and diffuse transmission. Correlation coefficients are gross space-time averages, limiting accuracy. Calculations have been checked against clear-sky data, and are considered accurate to about $\pm 10\%$. If I_{coll} is measured, that data could be used rather than the estimated clear-sky value. $T_{\text{coll,in}}$ is taken as $T_{\text{tank,meas}}$ when the tank is well-mixed. It can be hard to estimate in stratified tanks when a single mid-tank probe is used (three probes mid/hi/low are best for stratified, low-flow cases, with the low sensor taken as $T_{\text{coll,in}}$. Computation of $T_{\text{mains-in}}$ is provided, so formulae averaging it with the measured T_{tank} can be tested. T_{amb} for calculating useful energy gain is generally not measured; in the tool here one can linearly interpolate T_{amb} from estimates of $T_{\text{amb,max}}$ and $T_{\text{amb,min}}$. T_{amb} data can be used directly if available. ρ_{grd} is typically set to 0.2 for grassy foreground or asphalt, 0.3 for concrete, and 0.8 when fresh snow covers the ground.

TABLE 2: ANALYSIS INPUTS

Symbol	Parameter Definition	Data Source
System/site/test Inputs		
A_{coll}	Collector area	Label ¹ /Obs ²
$F_r \tau \alpha$	Optical gain constant	Label/SRCC ³
$F_r U_l$	Loss coefficient	Label/SRCC
b_o	Constant in IAM formula	Label/SRCC
V_{tank}	Tank Volume	Label/obs
H_{tank}	Tank Height	Obs/spec
R_{tank}	Tank insulation R value	Specs/obsrv
θ	Collector tilt & azimuth	Obs
L	Longitude	Map
Lat	Lat	Map
$T_{\text{amb,high/low}}$	Test lo/hi daytime temps	Met data/obs
ρ_{grd}	Foreground reflectivity	See text
$T_{\text{amb,month,high/low}}$	Monthly average min/max ambient temp	Met data, local obs
Data reduction inputs		
$(dT_{\text{tank}}/dt)_{\text{min}}$	Minimum dT_{tank}/dt for solar gain analysis	Trial and error
$t_{\text{beg}}, \Delta t_{\text{UA}}$	UA analysis window	Trial and error
ΔT_{min}	Min. ΔT for UA analysis	Trial and error

1) Label on the collector often lists collector parameters.

2) Obs = observation at the site

3) Solar Rating and Certification Corp., at www.solar-rating.org

The expected values of pump on/off times are taken as the start/end of the period where $dQ_{\text{coll,clr}}/dt$ is positive. No deadbands are accounted for. Inferred values of UA_{tank} are compared to expectation based upon 1-D calculation. U_{tank} is taken as $k_{\text{ins}}/L_{\text{ins}}$. The tank surface area A_{tank} is calculated based on inputs for V_{tank} and H_{tank} assuming a cylindrical tank. Because of typical uninsulated thermal shorts (piping, supports), the actual U value is expected to be $\sim 2X$ that of this simple estimate. Reverse thermosiphoning would show up as UA values much larger than this. It would be possible to gain further resolution of reverse thermosiphoning by valving off the collector for one night to establish the baseline for nighttime losses, then differencing that with results including the collectors.

3. EXAMPLES: VALIDATION AND DIAGNOSTICS

The methods above have been embodied in a spreadsheet tool available for download (6). In this section, the tool is used to analyze data from three different projects.

3.1 Building America test house: method validation

Detailed data from a residence in Colorado are being acquired under the Building America Program (9), and those data were used to validate the method. System

instrumentation is shown in Fig. 4. Because solar gain was measured, the solar gain inferred from tank calorimetry can be compared directly. Measured T_{env} and T_{amb} were used in the results shown here. Hourly data were used here.

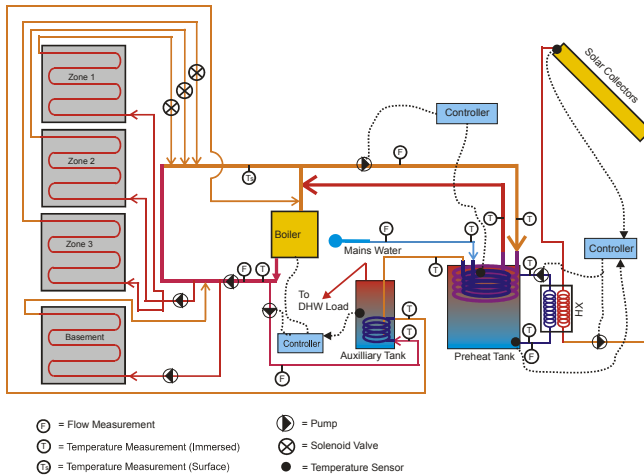


Fig. 4. Instrumentation schematic in the Solar Row #2.

Tank sensors were mounted under the insulation on the outside surface of the unpressurized pre-heat tank near bottom and top of the tank. The tank is well-mixed when the solar loop is operating, as shown in Fig. 5. When the solar pump is off and there is no space heating or draw, the tank bottom decays more rapidly than the top of the tank. Possible causes include: convection currents off the tank sides/thermal shorts, ground thermal shorts at bottom supports, or small night thermosiphoning (although flow at night always read zero in the storage-side heat exchanger loop). When the pump is off and there is space heating, the top/bottom sensors converge, diverging again when the space heat is turned off. Similar behavior is indicated upon large draw. It is believed that this mixing is caused by apparently-strong convection currents set up when there is a large heat extraction from the tank.

In Fig. 6, the predicted solar gain (yellow curve) is compared with the inferred solar gain (blue circles) over eight days corresponding to Fig. 5a. It can be seen that some days (2nd day), there are no measured points (indicative of irradiance too low to start pumps), and partly-cloudy days show gain below the clear-day values. Predictions vary in peak height (e.g., clear-day curve for day 2 lower than clear-day curve day 3) because the collector inlet temperature (taken as the lower of the tank sensors) varies, which causes efficiency and net solar to vary. The 5th and 6th days are clear days, and the model and measurement agree very well.

Measured solar gain is computed as flow- ΔT across the tank-side heat exchanger loop. This value is compared with the inferred gain $C_{tank}dT_{tank}/dt + dQ_{loss}/dt$ in Fig. 7. It can be seen that the correlation is good. For all data, the regression

line for inferred gain $C_{tank}dT_{tank}/dt$ vs. direct measurement of the gain as flow $\cdot\Delta T$ has slope of .9 and $R^2 \sim .8$. Disagreement is expected due to neglect of system mass, undetected draws, and errors in tank loss calculations. These data validate that tank surface temperature data is sufficiently accurate for inferring fluxes in the tank.

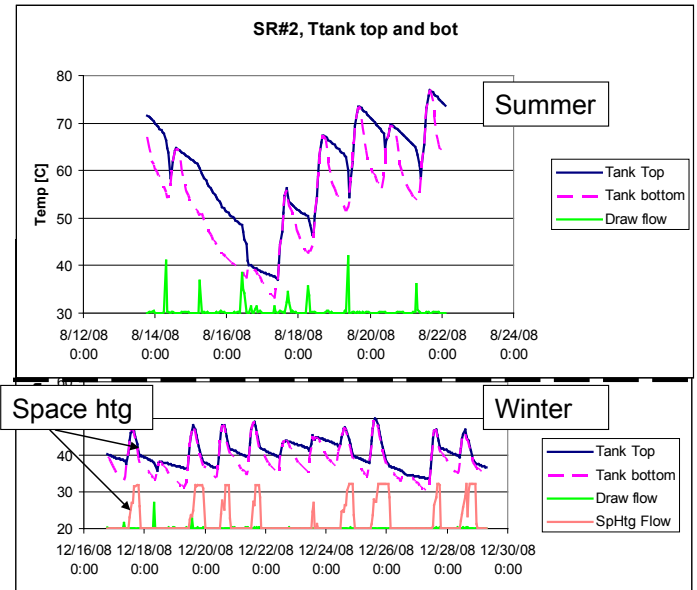


Fig. 5. Summer (top) and winter (bottom) T_{tank} in Solar Row Unit #2. Draw and space heating flows are also shown.

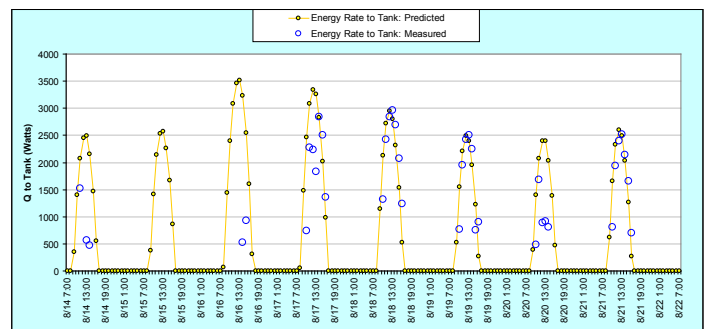


Fig. 6. Predicted clear-day solar gain (yellow curve) vs. the measured solar gain (blue circles).

UA_{tank} is shown for the entire data set in Fig. 8. Measured T_{env} data was used. It can be seen that during summer the inferred UA_{tank} is quite close to the estimated value based upon a 1-D calculation, validating the UA inference. It is unusual to have agreement this close, due to un-insulated thermal shorts (piping/valving). Typically, the measured UA is $\sim 2X$ the 1D estimation. The result here indicates that the thermal shorts are reasonably well-insulated. Note that during winter, the UA calculations will usually include periods with space heating load, so anomalously-large UA values result, as seen in Fig. 7.

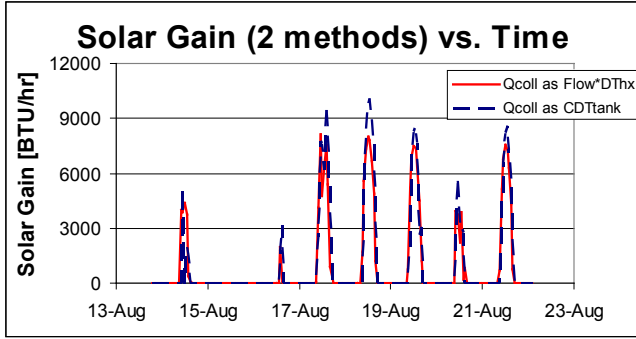


Fig. 7. Solar gain as measured by $C_{\text{tank}}\Delta T_{\text{tank}}$ and as $\text{Flow}_{\text{hx}}\Delta T_{\text{hx}}$ vs. time. Good agreement is seen.

3.2 SWH diagnostics in New York

Temperature and inferred flux for four days of data for a 64 ft² residential system are shown in Fig. 9. These data alone indicate functioning energy delivery: the unit warms up significantly on some days. Only two draws appear, both in the morning. Fig. 10 shows observed vs. calculated gain. Flux comparisons indicate that the unit is gathering most of the expected energy. Fig. 11 indicates inferred and calculated pump on/off times. The inferred start times on the first two days correspond reasonably to predicted values. Days 3 and 4 are evidently cloudy, but show shut-down close to expected times. By comparing *rates*, 38 data points were attained, as opposed to essentially 2 points using the daily total method in (3). With rate comparisons, good conclusions can be reached with only several days of data; one day of data under mostly-clear conditions is sufficient in the extreme.

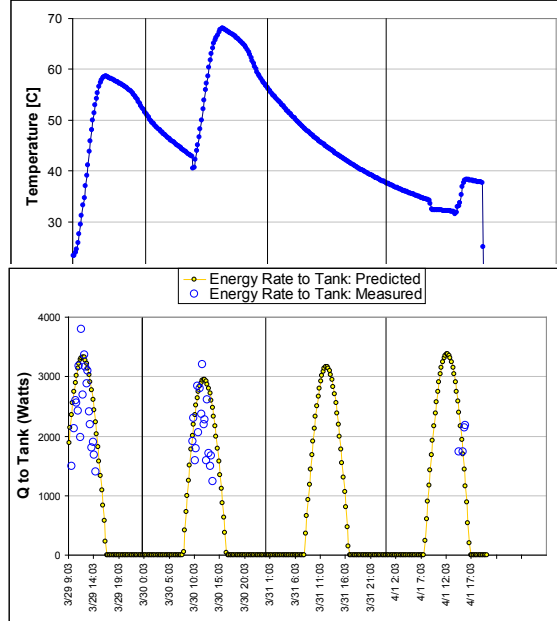


Fig. 9. Temperature and solar flux (computed and measured) for 4 days for a small system in New York.

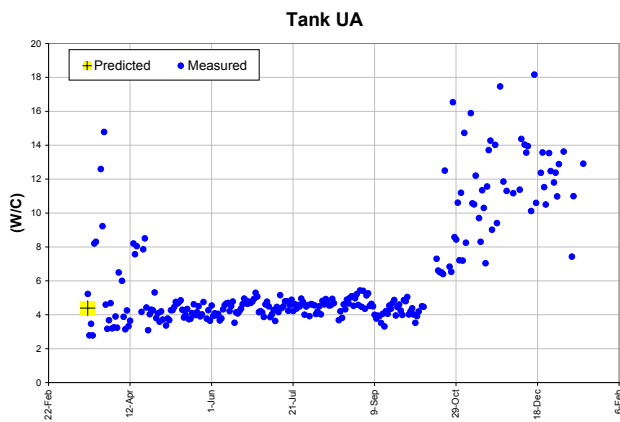


Fig. 8. Tank UA on successive nights, with value during summer near the 1-D calculation.

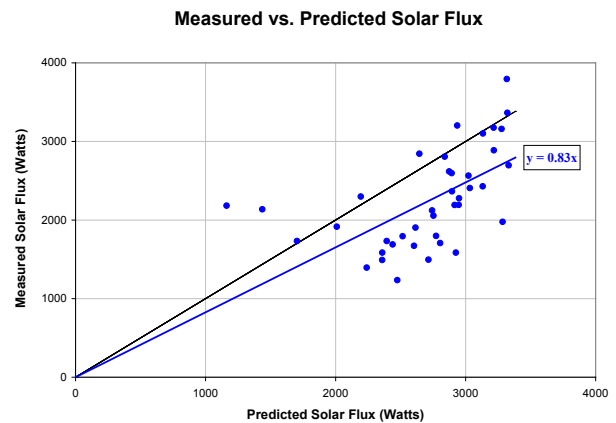


Fig. 10. Measured vs. predicted solar flux for a residential system in upstate New York.

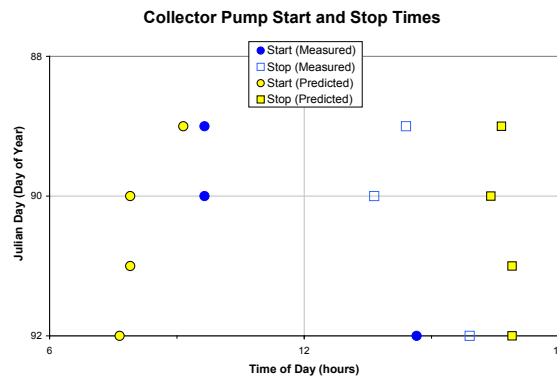


Fig. 11. Pump start/stop times, predicted and inferred.

A large SWH at Saranac Lake, NY on a 9-story multi-family building was monitored, with schematic in Fig. 12, and collectors and tank shown in Fig. 13. The system has 48 4X8 collectors ($A_{net} = 1368 \text{ ft}^2$) in 8 strings in series and up to 8 collectors in a single string. The pressurized storage volume is 1389 gal. The piping run is about 250 ft. A schematic of the system is shown in Fig. 12. It is a glycol system with external doubly-pumped load-side heat exchanger. This case illustrates that the method applies to large-scale systems. However, there are additional issues with frequent, relatively-small daytime draws that reduce accuracy (unless draw data are taken), and piping runs in large systems that significantly impact losses.

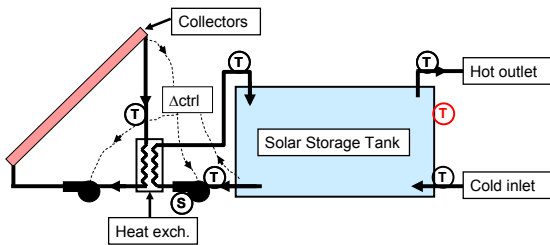


Fig. 12. Schematic of the Saranac Lake SWH. Temperatures are indicated by “T”, status with “S”. The red temperature sensor on right side of tank wall was used for calorimetry.

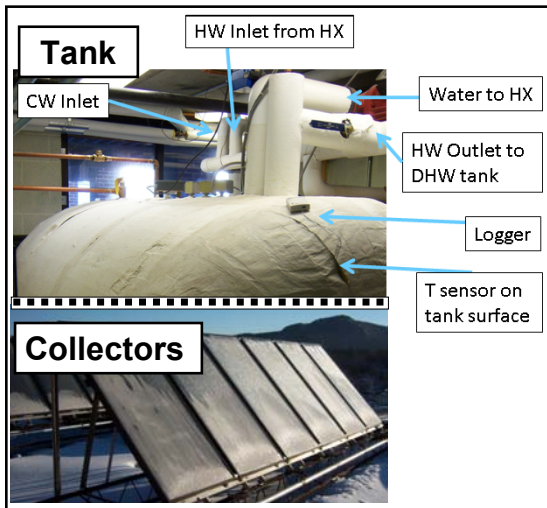


Fig. 13. Saranac Lake SWH. *Top*: Tank in the basement, showing logger/sensor position. *Bottom*: one string of six collectors in parallel on the roof.

Collector gain and loss coefficients as printed on the collector labels are given in Table 4. The multipliers for the off-test flow rate, series connections, piping, and the heat exchanger penalty (8) are also shown in the table. ϵ_{hx} was estimated at 0.5. The largest correction is a factor of 1.72 for piping. The corrections reduced the gain by 10% and increased the losses by 84%. The system corrections to collector parameters are especially important for large SWH.

TABLE 4: CORRECTIONS TO SOLAR GAIN

Gain: orig. ¹	Loss: orig. ²	F_{flow}^1 [-]	F_{array}^1 [-]	F_{pipe}^1 loss	F_{pipe}^1 gain	F_{hx}^1	$F_{gain: corr}^{1,3}$	$F_{loss: corr}^{2,3}$
.781	.8	1.01	0.95	1.72	.995	.91	0.712	1.26

- 1) Unitless; label value
- 2) Units of Btu/hr-ft²-°F; label value
- 3) Corr = Correction after applying the four factors.

Fig. 14 shows the tank temperatures and solar gains for an 8 day stretch during Oct. 2008. The temperature data show a clear rise mid-day on four of the days. The corresponding solar gain is shown as blue circles in the bottom part of Fig. 14. It can be seen that the collected energy is ~60% below the expectation. Fig. 15 shows the pump start/stop times. The inferred values indicate late start-up each morning. Piping/fluid mass warmup and consistent morning clouds in the cloudy area could both be factors.

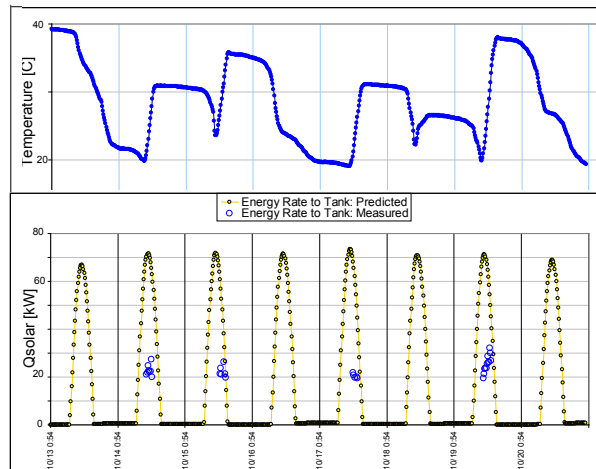


Fig. 14. Tank temperature and solar flux (computed and measured) for 8 days for a large system in New York.

Additional data channels can help to resolve uncertainties that arise from using a single sensor. The channels shown in Fig. 12 in black font were installed to help explain the 1-channel calorimetry data, data shown in Fig. 16. The tank data clearly show that the tank is well-mixed once the heat exchanger pump turns on. This was surmised based upon the specified 50 gpm flow rate at the heat exchanger (~2.3 turnovers/hr). The data also indicate that there were draws all day long, because T_{mains} never rose above 40 °F. Only for ~2-5 AM did T_{mains} show any rises toward T_{env} . Draw energy lowers net energy, so its effect is indistinguishable from “low” $Q_{dot,solar}$. There are few times without draws and they cannot be seen as discrete events, as occurs with draws in single-family data, reducing accuracy. With large, multi-family systems, draw flows should be monitored and subtracted out of the energy balance, if a valid comparison with the expected solar gain is desired.

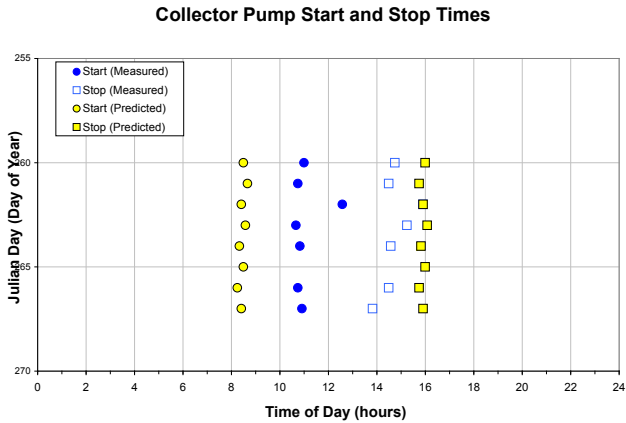


Fig. 15. Pump start/stop times (inferred and calculated) for the Saranac Lake multi-family SWH.

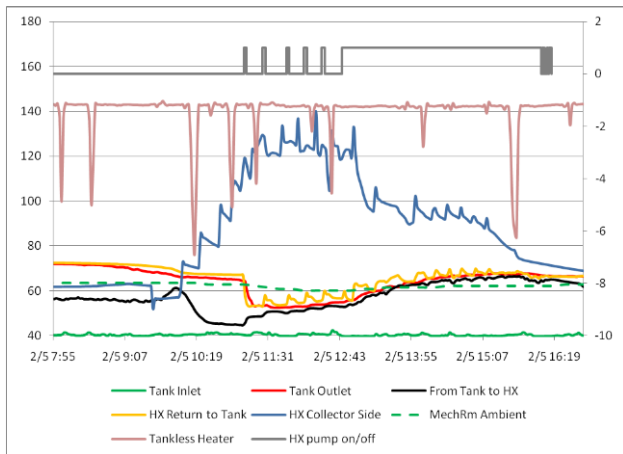


Fig. 16. Multi-channel data for one day on the multi-family Saranac Lake SWH.

3.3 SWH Field Testing using tank as calorimeter

Field monitoring was conducted on ten installations of a new SWH to detect and resolve any malfunctions (10). Inoperative systems were easily detected in two cases, as $T_{\text{tank}}(t)$ never fluctuated more than a few °C. The circulation system failures were identified and fixed, with appropriate changes in the system manuals. In cases where pumps run appropriately but there is no actual flow, one can be fooled into thinking the SWH is functioning properly.

Fig. 17 shows data from a properly-operating system. The temperature data show that the system is collecting energy properly. However, the flux data in Fig. 17b shows that the system energy collection is quite low in morning. Fig. 18 shows that the pump operates as expected, pointing to morning shading issue; this can also be seen directly in the temperature data in Fig. 17a, evident as the relatively slow temperature rise in the mornings.

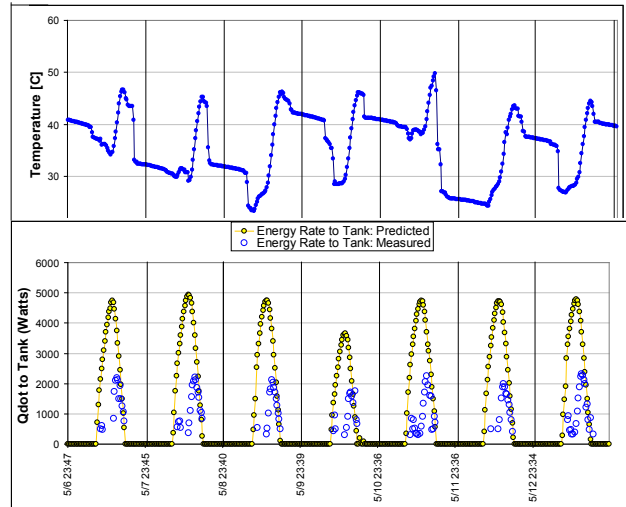


Fig. 17. Tank temperatures (top), and measured and computed clear-day net power to tank (bottom) for SWH #9.

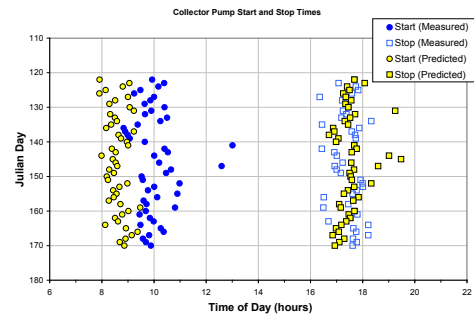


Fig. 18. Pump start/stop times for SWH #9.

Data on several of the systems showed unexplained early shut-down of the pump. Two examples are shown in Fig. 19, where shutdown appears early every day. This behavior is being investigated, possibly related to the collector outlet temperature sensor being “glued” to the roof near the collector, rather than stably fixed under insulation on the outlet manifold.

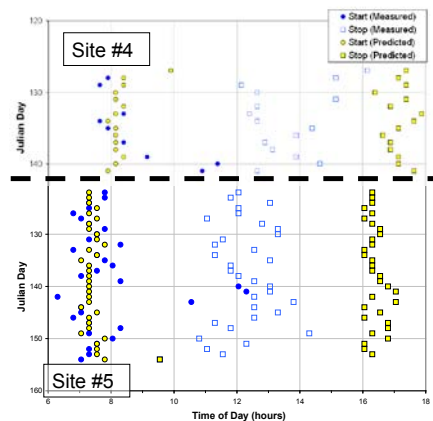


Fig. 19. Pump start/stop times for two SWH in Florida.

4. CONCLUSIONS

The simple calorimetric method here appears useful for diagnosing SWH operations. It works well when the solar tank is well-mixed during solar operation, so that the measurement at one point on the wall represents the average tank temperature. With highly-stratified systems, multiple sensors must be used to get a more-accurate measure of $T_{\text{tank,avg}}$. An available spreadsheet tool (6) was developed that embodied the analysis method. The method was validated with direct solar gain data, with high correlation between direct and inferred solar gain ($R^2=0.8$). Malfunctioning systems are easily detected because fluctuations in T_{tank} are very low. Shading and control issues with operating systems can be detected. The method could be embedded in controllers for continuous diagnostics, and could be used in a large-scale program to identify non-performing systems and gather reliability data.

Future software work includes: i) producing a user-friendly version of the software if there is sufficient interest; ii) investigating large-scale mail-in projects in collaboration with SWH maintenance and repair firms; and iii) potential collaboration with controls manufacturers.

5. NOMENCLATURE

Symbols

A	Area
c_p	Heat capacity at constant pressure
C	Capacitance of tank (water + walls + instruments)
F	Heat removal factor of the collector
K	Incidence angle modifier
Q	Thermal energy
t	Time
T	Temperature
U	Unit area conductance
α	Short-wave absorptivity of the absorber
Δ	Difference
ε	Effectiveness of the heat exchanger
θ	Orientation vector (embodies both tilt and azimuth)
τ	Transmission of the glazing(s)

Subscripts

amb	Ambient
avg	Average
beg	Beginning of a time interval
clr	Clear day, assumed for expectation calculations
coll	Collector
dot	Denotes time derivative of the variable
end	End of a time interval
env	Environment of the tank
hx	Heat exchanger
i	Index for data points

IAM	Incidence angle modifier
loss	Loss from the tank walls
mod	Model
n	Normal to the collector plane
r	Heat removal
tank	Solar storage tank
useful	Useful energy exiting the collector

6. ACKNOWLEDGMENTS

The authors acknowledge funding from the U.S. Department of Energy's Buildings Technology Program, Innovative Systems Program, Solar Heating and Cooling sub-program, managed by Bob Hassett.

7. REFERENCES

1. Burch, Jay, "Homeowner Tests for Diagnosing Solar Water Heaters", 1996 draft report, NREL. Available at ftp://ftp.nrel.gov/pub/solar_waterheat-out/tank_calorimetry/
2. ASHRAE 1991, "Installation Manual for Solar Water Heating Systems", Appendix G. Available at <http://www.solar-rating.org/commercial/guidelines.htm>.
3. Burch, Jay, Xie, Y. and Murley, C., "Field Monitoring of Solar Domestic Hot Water Systems Based on Simple Tank Temperature Measurement", Proc. American Solar Energy Society Annual Conference, 1995, San Francisco, CA
4. Buckles, W. E., "Solar Term Monitoring and Performance Evaluation of Solar Domestic Hot Water Systems", Masters Thesis, University of Wisconsin, Solar Energy Lab, 1983.
5. Barker, Greg, Burch, J., and Hancock, E., "Field tests of a Short-term Monitoring Method for Solar Domestic Hot Water Systems", Solar Eng 1990, Miami, FL.
6. The tool *SWH_diagnostics.xls* is available at ftp://ftp.nrel.gov/pub/solar_waterheat-out/tank_calorimetry/
7. Burch, J., Shoukas, G, Brandemuhl, M, and Krarti, M., "Test and Rate Methods for Thermosiphon solar water heaters", Proc. American Solar Energy Society Annual Conference, 2006.
8. Duffie, John, and Beckman, W., "Solar Engineering of Thermal Processes", 2nd Edition, John Wiley and Sons, NY, NY, 1992.
9. Paul Norton, Magnusson, L., Hendron, B., Hancock, E., and Barker, G. "Building America Field Test Report: NREL/Wonderland Development: Wonderland Near-Zero Energy Row Houses- Boulder, CO", available at ftp://ftp.nrel.gov/pub/solar_waterheat-out/tank_calorimetry/.
10. Nathan Aronson, Rubio, M., "Final report on Field Monitoring of 10 Drainback Systems", report to NREL from FAFCO, Inc., available from the first author.

REPORT DOCUMENTATION PAGE

Form Approved
OMB No. 0704-0188

The public reporting burden for this collection of information is estimated to average 1 hour per response, including the time for reviewing instructions, searching existing data sources, gathering and maintaining the data needed, and completing and reviewing the collection of information. Send comments regarding this burden estimate or any other aspect of this collection of information, including suggestions for reducing the burden, to Department of Defense, Executive Services and Communications Directorate (0704-0188). Respondents should be aware that notwithstanding any other provision of law, no person shall be subject to any penalty for failing to comply with a collection of information if it does not display a currently valid OMB control number.

PLEASE DO NOT RETURN YOUR FORM TO THE ABOVE ORGANIZATION.

1. REPORT DATE (DD-MM-YYYY) April 2009		2. REPORT TYPE Conference Paper		3. DATES COVERED (From - To)	
4. TITLE AND SUBTITLE Diagnosis of Solar Water Heaters Using Solar Storage Tank Surface Temperature Data			5a. CONTRACT NUMBER DE-AC36-08-GO28308		
			5b. GRANT NUMBER		
			5c. PROGRAM ELEMENT NUMBER		
6. AUTHOR(S) J. Burch, L. Magnuson, G. Barker, and M. Bullwinkel			5d. PROJECT NUMBER NREL/CP-550-45465		
			5e. TASK NUMBER SH072003		
			5f. WORK UNIT NUMBER		
7. PERFORMING ORGANIZATION NAME(S) AND ADDRESS(ES) National Renewable Energy Laboratory 1617 Cole Blvd. Golden, CO 80401-3393				8. PERFORMING ORGANIZATION REPORT NUMBER NREL/CP-550-45465	
9. SPONSORING/MONITORING AGENCY NAME(S) AND ADDRESS(ES)				10. SPONSOR/MONITOR'S ACRONYM(S) NREL	
				11. SPONSORING/MONITORING AGENCY REPORT NUMBER	
12. DISTRIBUTION AVAILABILITY STATEMENT National Technical Information Service U.S. Department of Commerce 5285 Port Royal Road Springfield, VA 22161					
13. SUPPLEMENTARY NOTES					
14. ABSTRACT (Maximum 200 Words) Based on the tank energy balance, net gain into the solar storage tank can be inferred from the time derivative of the average tank temperature. Using temperature at the tank wall under insulation as a surrogate for fluid temperature, sensor mounting is simple and the inferred gains are useful for solar water heater (SWH) diagnostics. Positive daytime gain is compared to solar gain computed from site-specific parameters for an assumed clear day. The solar storage tank loss coefficient is inferred from temperature decay at night and is compared to the value computed from tank description. Larger draws are evident as sharp drops in storage temperature. Analyses are embodied in a tool validated against directly measured gains. Inoperative single-family SWHs are easily detected, signaling the need for repair. Detection of system control issues and shading are exemplified. In large multi-family systems, frequent day-time draws will bias the comparison to expected solar gain.					
15. SUBJECT TERMS PV; solar water heater; storage tank; diagnostics; temperature data; solar gain; loss coefficient;					
16. SECURITY CLASSIFICATION OF:			17. LIMITATION OF ABSTRACT UL	18. NUMBER OF PAGES	19a. NAME OF RESPONSIBLE PERSON
a. REPORT Unclassified	b. ABSTRACT Unclassified	c. THIS PAGE Unclassified			19b. TELEPHONE NUMBER (Include area code)